

The Egyptian International Journal of Engineering Sciences and Technology

https://eijest.journals.ekb.eg/

Vol. 52 (2025) 76-90

DOI: 10.21608/eijest.2025.336089.1306



Thermal Characteristics Comparison between Normal Diffusion Flame and Concentric Inverse and Normal Diffusion Flame Burners in Ribbing Furnace

Ashraf Kotb^a*, Hany Saad^b

^aAssociate Professor – Mechanical Power Department ^bProfessor – Mechanical Power Department Ain Shams University – Faculty of Engineering – Cairo – Egypt

ARTICLE INFO

Article history:

Received 15 November 2024 Received in revised form 15 November 2024 Accepted 18 January 2025 Available online 18 January 2025

Keywords:

Inverse diffusion Flame Radial Ribs Normal Diffusion Flame This investigation is accomplished experimentally to study the use of two different shapes of annular-ribs (triangle and square shape) on the flowrate of heat transfer, and combustion characteristics for both normal diffusion NDB and concentric inverse and normal diffusion CINDF flame burner. The rate of heat transfer from LPG fuel flames in a cylindrical horizontal water-cooled furnace when the fuel is injected in the furnace axially was measured. In addition, A mathematical model for calculating the distribution of the local heat transfer rate from the flame to the furnace wall segments is used in the present study to compare both the measured value with calculated one. The results showed that; annular-ribs increases heat transfer across the furnace walls. Also, using triangle rib increases heat transfer and produces the minimum CO emission than the squared one in both NDB and CINDF burners. Also there are good agreements between the measured and calculated heat transfer to the furnace walls by using the analytical model.

1. Introduction

A lot of studies on flames were conducted to the development of technology for improving combustion efficiency and to the reduction of pollution associated with combustion processes [1, 10, 24]. Recent research interests include the development of flame configurations, enhancement of the heat transfer rate, reduction of combustion emissions and the soot formation analysis [3, 10, 23, 24].

ABSTRACT

Combustion flames from gaseous fuels take many forms: premixed-flames, diffusion-flames, Inverse-diffusion-flames (IDF) and triple-flames. Premixed-flames take place when the fuel and oxidizing agent are mixed before the flowing to the combustion space. Diffusion-flames take place when the fuel and oxidizing agent are separately flowing to the combustion zone. The reaction zone is located at an interface where the fuel and oxidizing agent mix in chemically correct proportions. Diffusion flames are named because the mixing process is controlled by diffusion between oxidizer and fuel, [5, 11].

Diffusion flames may take a Varity of forms such as fuel jet-flames, opposed jet diffusion-flames, axial coflowing jet diffusion flames or shear layer diffusion flames. Premixed-flames are cleaner and burn more intensely; but the working range is narrow because the flash-back or liftoff of the flames, [23] another form of flame is the triple flame which forms with three coaxial streams of fuel and air. This flame type is a combination between non-premixed and premixed flames.

In this flame two sides are formed, the first one is a rich-premixed-flame which is formed in rich fuel side while the other one is the lean-premixed which is formed in the lean side [17, 20, 21, 25].

Heat transfer in furnaces enhancement can be achieved by increasing coefficient of heat transfer, transfer area and temperature difference. Increasing the coefficient of heat-transfer could be by different methods, increasing the turbulence intensity, using swirl burners, using radial ribs, and WVGs (winglet type vortex generators). The vortex flow generation using these methods helps to increase the heat-transfer coefficient [6]. Many numerical and experimental studies have been conducted to investigate the effect of ribs on the flow of heat-transfer and combustion improvement including their Shapes, sizes, and placement location. [6, 9]

Many attempts [10, 23, 24] studied the performance of square ribs, triangular ribs, and semi-circular ribs. They reported the heat-transfer performance using the square and rectangular ribs has increased. A numerical study on heated section square duct including staggered V shape ribs is conducted [6]. They concluded the convection heat transfer is improved by the vortex flow. Also increasing the ribs height enhance the convective heat transfer as the vortex strength increased while the pressure-drop increased.

Caliskan [8] investigated the effect of V-ribs for air jet impingement on heat transfer and fluid behavior. They found that using V-shaped ribs increases the heat-transfer coefficient comparing with the smooth surfaces.

Kamali and Binesh [18] studied the effect of friction and turbulent heat-transfer with various shaped ribs fixed on one wall using square duct. Two trapezoidal one with decreasing height and the other with increasing height (both in the flow-direction), triangular and Square are used in the simulations. The simulation results showed that the distribution of the heat-transfer coefficient of the intermediate rib were affected by the rib shape strongly. In addition to using trapezoidal ribs with decreasing height in the flow-direction enhance the pressure drop with higher rate of heat-transfer than other shapes. Hisham Elmouazen et. Al. [14], studied the effect of different 3 V shaped ribs in hydrogen rocket engine chamber on heat-transfer characteristics. They founds that using V-shape ribs increase the convection heat-transfer coefficient value and improving the engine thermos hydraulic characteristics by 23% compared to using channels with smooth cooling.

Also, using ribs in combustion furnaces improves the heat-transfer performance and enhances the combustion performance. SiliangNi et. Al. [22] investigated the effects of double ribs on NOx emissions and energy efficiency on NH₃-powered micro-combustor. They reported that using double ribs reduced the NOx emissions and increased thermal performance.

The effect of using the annular ribs in premixed flame burner was studied by Amr et. Al. and Ahmed Al. [2, 26]. They concluded that using ribs in combustion furnaces increases the heat transfer rate while the effect of triangle shape is greater than square one on the heat flux, greater than the effect of the squared one.

Form previous studies, many research were conducted to find the effects of ribs shape, number, size, location and the ratio of pitch/rib height on friction and heat-transfer results inside tubes and square channels. The aim of the work is to study the effect of annular-ribs with two different shapes (triangle and square) with the same cross-sectional area on the combustion performance and the rate of the heat-transfer by using two different forms of burners, one using normal diffusion flame burner (base case) and the other using CINDF flame burner throughout a water cooled horizontal cylindrical furnace of gaseous fuel. The location of the radial rib and the equivalence ratio Φ are fixed in during all experiments. In addition to establish an analytical model to calculate the heat transfer from the flame to furnace wall.

2. Test rig and experimental procedure:

A comparison is carried out experimentally to investigate the effects of annular ribs on the combustion emissions and the heat-transfer for both pre-mixed and

concentric inverse and normal diffusion flames (CINDF) gaseous flame through a water cooled horizontal cylindrical Fig. 1 shows the schematic diagram of the experimental test rig. This test rig is the same used by both Amr et. Al. and Ahmed, et. [2, 26]. Using the same furnace with the same dimension after adding some modification to measure the heat transfer from the furnace as described later. Also, they used premixed and triple flame burners in their study while in this study the burners used normal diffusion flame and concentric inverse and normal diffusion burners (CINDF). The fuel is liquefied petroleum gas, LPG (60% C_4H_{10} and 40% C_3H_8 by volume) according to MISR Petroleum Company (EN 589). The fuel low heating value (LHV) is equal to 105 MJ/m³. The fuel used is storage at (5000 ±100) Pa in a steel cylinder to feed the burner. To adjust the fuel flow rate, a regulator pressure valve is installed in the fuel cylinder exit and keeps the exit LPG fuel pressure to the burners constant for all experiments at 3000 Pa. The air is flowing to the burners by pressurized tank of air. The air and fuel are forced to the normal diffusion flame burner while the supply air is divided into two streams to form the two flows jet for the CINDF flame burner as shown in Fig. 2. For both burners the crosssectional area for both fuel side and air sides are the same. To control and measure the air flow rate in such a flame, two ball valves are inserted in each line with two calibrated air flow meters. Water-cooled furnace has been designed to facilitate the measurements of the flame- temperature along the furnace, heat flux and composition of combustion products.

The furnace consists of two co-axially pipes have inside diameter of 10.5-cm and outside diameter of 15-cm with 0.6 m long. The annular space between the two concentric pipes represents the cooling water jackets divided into 6 non-symmetric axial segments to make the ability to indicate the local rate of the heat-transfer from the different flames, as shown in Fig. 1. The segments width is 10 cm for the first 3 segments and 15 cm for the other 3 segments. Flame inspection holes 10 mm diameter are fitted in the middle of each cooling segment in horizontal plane to give the ability to measure the flame-temperature and gaseous concentrations along the furnace length, as shown in Fig. 1. As a result, the axial distance from the burner tip to inner burner diameter ratio (X/d) for these holes are 0.47, 1.42, 2.38, 3.5, 5, and 6.4 respectively.

In this work; two sectional areas of annular ribs (square-triangular) are used. The annular rib location is fixed at X/d equal to 0.95 during all experiments as it is the end of the first segment. Fig. 3 shows the squared, triangle ribs, dimensions and geometry.

The flame temperature in furnace was measured using type S (Pt-Pt Rh 10%) thermocouples with a wire diameter 0.1 mm and bead-size about 200 μ m to reduce the flame disturb during temperature measurement. The radiation loss was corrected according to Bradly [7]. On dry basis, the gas emission is reported using calibrated gas analyzer in the combustor exit. To fulfill the uncertainty analysis [12], each reading was recorded 3 times, and the average value is calculated as reported by Kline [19].

The precision of the air flow was ± 0.15 . Uncertainties in measurement of the flame-temperature are 2.7 % and 10.3 % for minimum and maximum temperature respectively with confidence level of 95 % and for CO emissions 9.5 % and 2.1 %, while for NO was 12.2 % to 2.2 %, respectively.

To verify the accuracy of the measurements the total energy balance of the furnace needs to be stated including the heat goes with the exhaust gases, such that the total heat transfer to the walls in addition to the heat goes with the exhaust gases are balanced with the fuel flow rate multiplied by the fuel heating value, for all the experiments.

3. Modelling and Simulation:

3.1 Calculation of the measured local wall heat flux along the furnace length:

The flux rate of heat is calculated by cooling water-jacket measurements. The inflow and outflow water temperature from each water jacket element is measured by calibrated thermocouple and these readings measured separately for each element. The cooling water flowrate is measured by a calibrated flow meter (digital type). The heat-flux at each element is calculated using the following equation:

$$q = \frac{\dot{m}_{w}.C.(T_{out} - T_{in})}{A_{segment}}$$
 (1)

Where

q: Heat flux $[W/m^2]$.

 \dot{m}_{w} : Water mass flow rate, [kg/s].

C : Specific heat (Water), [kJ/kg.°C].

 T_{out} : Water outflow temperature from the cooling segment, [${}^{\circ}$ C].

 T_{in} : Water inflow temperature to the cooling segment, [°C].

 $\mathbf{A}_{segment}$: Cooling water element surface area, [m²].

3.2 Mathematical Model for calculated local heat flux:

The heat flux distribution along a water-cooled furnace is a function of the flame characteristics and furnace dimensions. Flame characteristics are mainly functions of air to fuel ratio, fuel type, fuel injection rate and fuel-air mixing process. The flame characteristics include flame temperature and concentration of species such as soot and gases along the flame. A mathematical model is developed using the furnace dimensions and the flame characteristics to calculate the distribution of the heat flux to the furnace walls [13, 16].

3.2.1 Calculation of the theoretical local wall heat flux along the furnace length:

A mathematical model for calculating the heat transfer from the flame and the combustion products to the furnace wall which is based on the hypothetical long furnace described by Hottel and Sarofim [16] is used. In this model the long furnace is divided into small axial zones. For the long furnaces, the radiation in the axial direction is ignored. Also the zones are defined as well stirred zones at which either the partial pressure of any gas product or the flame temperature can be described by a single value, which is the average value across each section. In the present calculations, the furnace space is divided into a series of small four segments, which are considered as well stirred

zones. The heat flux which is absorbed by the furnace wall is defined as the sum of the heat transferred by radiation and by convection from the luminous flame and the combustion products to a unit area of the furnace wall, [13, 15]. The heat transfer by radiation to the furnace wall segment number (w,n) is the sum of the soot and gas radiation from the flame segment number (f,n) and more over the radiative heat transferred from the other flame segments which are located upstream and downstream the flame segment (f,n), as shown in Fig. 4, [11, 13].

To simplify the calculation of the heat transfer rate to the furnace walls from the luminous flame and the combustion products by the mathematical model which was developed by Hassanin [13] the following assumptions have been made:

- The flame temperature is represented by the measured average temperature across the furnace diameter in the measuring location, X/d, [16].
- Heat transfer by conduction between the wall segments is so small because of the very low temperature difference between the wall segments.
- The axial radiation between the flames segments is neglected, [16].
- The enthalpy difference of the unburned hydrocarbons between the inlet and outlet of each segment is neglected, i.e. the change of the enthalpy of the unburned hydrocarbons across each flame segment is small.
- Net radiant heat exchange between wall segments is absent since the wall temperature variation is quite small.
- The fourth power of the wall temperature is neglected compared to the fourth power of the flame temperature in calculation of the radiation from the flame segments to the furnace wall segments.
- It is also assumed that the luminous flame fills the whole cross section of the tube to calculate the shape factor between the flame segments and furnace walls as detailed below.
- The convective heat transfer coefficient between combustion products and the inner furnace wall is nearly constant along the furnace length, and assumed to be 4 W/(m².°C), [4, 13].
- The wall emissivity is assumed to be uniform along the furnace length and equal 0.8, [11].
- The flame emissivity plays an important role in the values of the heat transfer from flame to the furnace walls. It was found that the emissivity of the liquid fuel flame has a peak value close to the burner outlet and decrease to a nearly constant value in the rest of the flame. An estimated average value of the flame emissivity is used in calculations based on the previous work, [4, 13].
- In the non-luminous zones, the gas emissivity is calculated by using the carbon dioxide and water vapor concentrations calculated from chemical equations. From the calculations it was estimated that the value of the gas emissivity which is calculated is about 0.1.
- In order to simplify the solution, the effect of reflection and re-reflections from the wall

segments to the incident radiation from the flame is neglected.

The mathematical model for calculating the heat transfer from the luminous and non-luminous flame is used. The heat transferred to the furnace wall segment number (w,n) from flame segment (f,n) by radiation is calculated by using the following equations:

$$Qr_{f,n\to w,n} = A_{w,n}\sigma \left[\frac{T_{f,n}^4 - T_{w,n}^4}{\left(\frac{1}{\mathcal{E}_{w,n}} - 1 + \frac{1}{\mathcal{E}_{f,n}}\right)} \right]$$
(2)

From the above assumptions $T_{f,n}^{4} >> T_{w,n}^{4}$, then the second term of the previous equation can be neglected, and equation number (2) will be simplified to:

$$Qr_{f,n\to w,n} = A_{w,n} \sigma \left[\frac{T_{f,n}^4}{\left(\frac{1}{\mathcal{E}_{w,n}} - 1 + \frac{1}{\mathcal{E}_{f,n}}\right)} \right]$$
(3)

And the radiative heat transferred from the flame segments number (n-1), (n+1), (n-2) and (n+2) upstream and downstream the wall segment number (w,n) are calculated by the following relations:

$$Qr_{f_{n+1}\to w,n}=A_{f}.\ (F_{f,n+1\to w,n}\).\ (\ \epsilon_{f})_{n+1}.\ (1\text{-}(\epsilon_{f})_{n}).\ (\epsilon_{w})_{n}.\sigma.\ (T_{f}^{\ 4})_{n+1}$$

$$Qr_{fn-1\to w,n} = A_f. (F_{f,n-1\to w,n}). (\epsilon_f)_{n-1}. (1-(\epsilon_f)_n). (\epsilon_w)_n.\sigma. (T_f^4)_{n-1}$$
(5)

$$\begin{array}{lll} Qr_{fn+2\to w,n} &= A_{f\cdot} \ (F_{f,n+2\to w,n} \). \ (\ \epsilon_f)_{n+2}. \ (1\text{-}(\epsilon_f)_n). \ (1\text{-}(\epsilon_f)_{n+1}). \\ (\epsilon_w)_n.\sigma. \ (T_f^{\ 4})_{n+2} & \\ \end{array} \eqno(6)$$

$$\begin{array}{l} Qr_{fn\text{-}2\to w,n} = A_f. \ (F_{f,n\text{-}2\to w,n} \). \ (\ \epsilon_f)_{n\text{-}2}. \ (1\text{-}(\epsilon_f)_n). \ (1\text{-}(\epsilon_f)_{n\text{-}1}). \\ (\epsilon_w)_n.\sigma. \ (T_f^{\ 4})_{n\text{-}2} \end{array} \eqno(7)$$

The heat transfer by convection between the flame segment number (f,n) and wall segment number (w,n) is calculated by the following relation:

$$Qc_{f,n\to w,n} = A_{w.} h_{c.} (T_{f,n} - T_{w,n})$$
 (8)

Then the total heat transferred to the wall segment number (w,n) from flame segment number (f,n) and from the two upstream and downstream segments to flame segment number (f,n) is given by the following relation:

$$\begin{aligned} Qt_{f\rightarrow w,n} &= (Qr_{f,n\rightarrow w,n} + Qc_{f,n\rightarrow w,n}) + Qr_{fn+1\rightarrow w,n} + Qr_{f,n+2\rightarrow w,n} &+ \\ Qr_{f,n-1\rightarrow w,n} &+ Qr_{f,n-2\rightarrow w,n} \end{aligned}$$

In equations ((4), (5), (6) and (7)) the view factor between the flame segment and wall segment is calculated by the equation number (10), which is used for two parallel discs, [31].

$$F_{1-2} = \left[\left[\left(\frac{D_2}{2D_1} + 0.5 \right)^2 + \left(\frac{X}{D_1} \right) \right]^{0.5} - \left[\left(\frac{D_2}{2D_1} - 0.5 \right)^2 + \left(\frac{X}{D_1} \right)^2 \right]^{0.5} \right]^2$$
(10)

The view factor between the flame area (A_f) and the peripheral wall segment area number (n) is determined from the view factor between two parallel circular areas with diameters, D_1 and D_2 , at a common perpendicular axis. The view factor between the two areas separating the flame segment number (n) from the two flame segments number (n+1) and (n-1), each of which is equals to (A_f) and face each other, and $D_1 = D_2$, can be calculated from equation (10) as shown in Fig 5.

Where, X is the axial distance between the two discs. The view factor between the flame segment number (n+1) and the wall segment number (n) is determined from the following relation:

$$F_{f,n+1\rightarrow f,n-1} + F_{f,n+1\rightarrow w,n} = 1$$

4. Results and Discussions:

The effect of changing the annular-rib shape on characteristics of combustion and heat-transfer was investigated. A comparison between flame temperatures, exhaust gas analysis and gas emissions are presented for squared and triangular cross-sectional shape of the annular rib for both normal diffusion flame NDB and CINDF flame burner. Also, the results are compared with no annular rib case. The rib location is fixed at X/d equal to 0.95. Also, the equivalence ratio Φ is constant for all experiments and equal to unity. The Equivalence ratio is between the chemically correct air/fuel ratio to the actual primary, (the

central air jet), air/fuel ratio (
$$\Phi = \frac{(A/F)_{stoic}}{(A/F)_{Actual}}$$

4.1 The effect of the annular-rib in case of NDB burner:

In this section the temperature distribution, exhaust gas analysis and heat transfer are investigated for both square and triangle ribs when using a NDB burner. The results are compared with the base line (without rib). The data collected at the same equivalence ratio and location for ribs. Fig. 6 represents the variation of the flame-temperature along the furnace for NDF /burner without and with insertion the square and triangle-edged ribs stoichiometric-combustion at the end of segment one (X/d equal to 0.95). From this Fig. the flame distribution along the furnace for triangle ribs is higher than using square one. Furthermore, there is a significant enhancement in temperature distribution after insertion of the edged ribs than without ribs. The maximum flame temperature is recorded at X/D = 1.42 with 1334°C for triangle ribs, 1230°C for square ribs and 1101 °C for baseline case.

Also, Fig. 7 represents the Variation of the heat-flux along the furnace for NDB burner at the same experimental condition. The Fig. illustrates that the heat-flux distribution without ribs is low compared with both types of ribs used. As shown from this Fig., the maximum heat flux is found at the same position of maximum flame temperature at (X/D = 1.42) for all cases. The maximum value of the heat-flux

was 2426.9, 2316.9 and 2194 W/m² for triangle, square and baseline case respectively. The percentage enhancement of heat-flux at this point is about 10.6% when using the triangle-edged rib while it is only 5.6% when using the square-edged rib.

From the above results it was found that the flame-temperature and heat-flux from flame when using ribs is higher than not using ribs case. This is because using ribs with different shapes produces a swirling motion and eddies performed due to presence of the solid part of these ribs which change the direction of the combustion flow gases increasing the flame stability and the residence time. As a result, enhances the combustion characteristics and increases the heat-transfer coefficient due to increase in the turbulence capacity. In addition, the ribs increase the surface-area which increases the heat-transfer.

Furthermore, the overall temperature and heat-flux using triangle ribs is higher than square ribs although the surface area for triangle rib is less than square one. this is because the swirl motion after using the triangular-rib is higher due to the length of the triangle side is longer than the length of the square side which increase the eddies effect in order to create more turbulence in the back flow region of the ribs in the flow direction. As a result, the turbulence effect for the triangle-edged rib is more than the square one which enhances the temperature and heat-flux.

In addition, the CO and NOx emissions are measured to indicate the effect of using ribs in NDB furnace on the exhaust gas analysis for the same experimental conditions as shown in Figs. 13 and 14. From this Fig. it is shown that, the CO emissions for using triangle rib lower than both with square ribs and without while, the NOx emission is higher as the overall temperature is higher when using triangle one. The CO emissions for using triangle rib is 342 ppm while for the square rib and without rib are 395 and 476 ppm respectively as shown in Fig. 13. And the NOx emission is higher when using triangle rib with 29.4 ppm value and 24 ppm for square rib and 22.3 ppm for baseline burner

4.2 The effect of the annular rib in case of CINDF flame burner:

The temperature distribution, exhaust gas analysis and heat transfer are investigated for both square-edged and triangle-edged ribs and without using ribs (base line) for using a CINDF flame burner in the furnace combustion. The data collected at the same equivalence ratio and location for ribs as in case of NDB burner.

Figs. 8 and 9 represent the variation of both the flame temperature and the heat flux along the furnace for CINDF flame burner without and with insertion the square and triangle-edged ribs for stoichiometric combustion at the end of segment one (X/d equal to 0.95). As shown in these Fig.s the flame distribution and heat-flux along the furnace for triangle ribs is higher than using square one and without using ribs. The maximum flame-temperature is achieved at X/D = 1.42 with $1461^{\circ}C$ for triangle ribs, $1367^{\circ}C$ for square ribs and $1290^{\circ}C$ for the case without rib as shown in Fig. 8.

Also, the maximum value of the heat flux was 3536.3, 2829 and 2438.8 for triangle, square and baseline case respectively. This means that the percentage of the

enhancement of heat flux at this point is about 31.9 % when using the triangle edged rib while it is only 15.9 % when using the square edged rib as shown in Fig. 9.

As discussed in case of using NDB flame it is found that the flame-temperature and heat-flux from flame when using ribs is higher than not using ribs case due to the production of the swirling motion and eddies performed due to presence of these ribs which improves the combustion characteristics and increases the heat-transfer. Also as discussed before the overall temperature and heat-flux using triangle ribs is higher than square ribs although the surface area for triangle rib is less than square one due to the higher level of turbulence in the back flow region of the ribs in the flow direction.

On the other hand, the CO and NOx emissions are shown in Figs. 13 and 14. From these Figs. it is shown that the CO emissions for using triangle rib is 414.6 ppm while for the square rib and without rib are 442.5 and 610 ppm respectively as shown in Fig. 13. And the NOx emission is higher when using triangle rib with 11ppm value and 9.4 ppm for square rib and 7.3 ppm for baseline burner as shown in Fig. 14.

4.3 The effect of the burner type using different annular ribs:

From this study it was found that using annular ribs increases the turbulent level near the walls which increases the flame stability and mixing effect between the air and fuel as shown in fig. 15. From this Fig. the streamline for the velocity field which produced from a numerical simulation is commissioned to reveal the reactive flow aspects of the investigated flame configuration with the same dimensions used in the experiments.

During these experiments it was found that the nominally the CINDF flame burner obtained at Φ =1, if compared with the corresponding NDB flame burner obtained at the same equivalence ratio Φ =1 as given in Figs. 10, 11 and 12, show flames of low soot and almost complete combustion with higher temperature-distribution and heat-flux to the furnace walls. This is noticed at all experiments with or without ribs.

Fig. 10 represents the variation of the flame-temperature along the furnace for both triangle and square rib at two different types of burners premise and CINDF one. From this Fig. it is shown that the flame temperature distribution for CINDF flame for both square and triangle ribs is higher than NDB flame. In addition, the heat-flux distribution for using CINDF flame also is higher for both triangle and square ribs as shown in Figs. 11 and 12.

In CINDF flame the jet of the outside air is getting into the burner by dividing concentrically the air to 2-parts around the fuel jet positioning to admission of the air internal portion and the fuel is interchanged. CINDF is inducing a strong turbulence due to increase in the central jet velocity which increases between the fluid layers the shearing strain as a result the air momentum increased. The fuel flow in the inner annular tube is entrained with high velocity resulting in a good mixing process which enhances the combustion efficiency than NDB. Furthermore, the CO emission is low compared with NDB. As a result, temperature distribution along the furnace axial direction

and the heat-flux are higher for CINDF than NDB as shown in Figs. 11 and 12.

4.4 Comparison between Measured and Calculated Heat Flux along the Furnace Length:

The local values of the calculated and measured heat flux along the furnace length are compared for both NDf and TDF at the same air to fuel ratio. The flame temperature, furnace wall temperature, estimated flame emissivity, air to fuel ratio and the furnace dimensions are used as input data to calculate the heat flux along the furnace length. The results are shown in Figs. 16 and 17.

These Figures show a comparison between the measured and the calculated heat flux transferred to the furnace walls. The heat flux increases sharply to a peak value at x/d equal to 1.42, in this location the calculated heat flux is slightly different from the measured values, due to the assumption of an average constant value of the flame emissivity, while it has a peak value close to the burner. In this work the length of the luminous flame was determined visually through the inspection holes. Along the non-luminous flame length and the calculated values of the local heat flux showed a good agreement with the experimental local heat flux values. The maximum difference between the calculated and measured local heat flux is about 7.51% for the premixed burner, while the maximum difference between the calculated and measured local heat flux is about 5.2% for the CINDF flame burner in the luminous flame zone. The low difference between the measured and calculated local heat flux in the luminous flame zone in this case is due to the small variation in the flame emissivity. For a good agreement between the measured heat flux and the calculated heat flux from this model, the actual variation of the luminous flame emissivity along the furnace is required.

5. Conclusions:

Using the annular-rib has a valuable effect on combustion characteristics, heat-transfer and emissions along the furnaces using both CINDF and NDB flame burner over similar combustors without using annular-ribs. The study showed the following:

- 1. Using the annular-rib increases the local heattransfer rates across the furnace wall.
- 2. Using annular-ribs enhances the flame-temperatures.
- 3. Using the triangle rib increases the heat-flux and the flame-temperature compared with squared one.
- 4. In case of using CINDF flame the percentage of the enhancement of heat flux at X/D = 1.42 is about 31.9 % when using the triangle edged rib while it is only 15.9 % when using the square edged rib.
- 5. In case of NDF the percentage of the enhancement of heat flux at X/D = 1.42 is about 10.6% when using the triangle edged rib while it is only 5.6% when using the square edged rib.
- 6. The local values of the measured heat flux along the furnace length and the corresponding values of the calculated heat flux, from the analytical model, are compared and found to be in good agreement for both NDF and CINDF one.

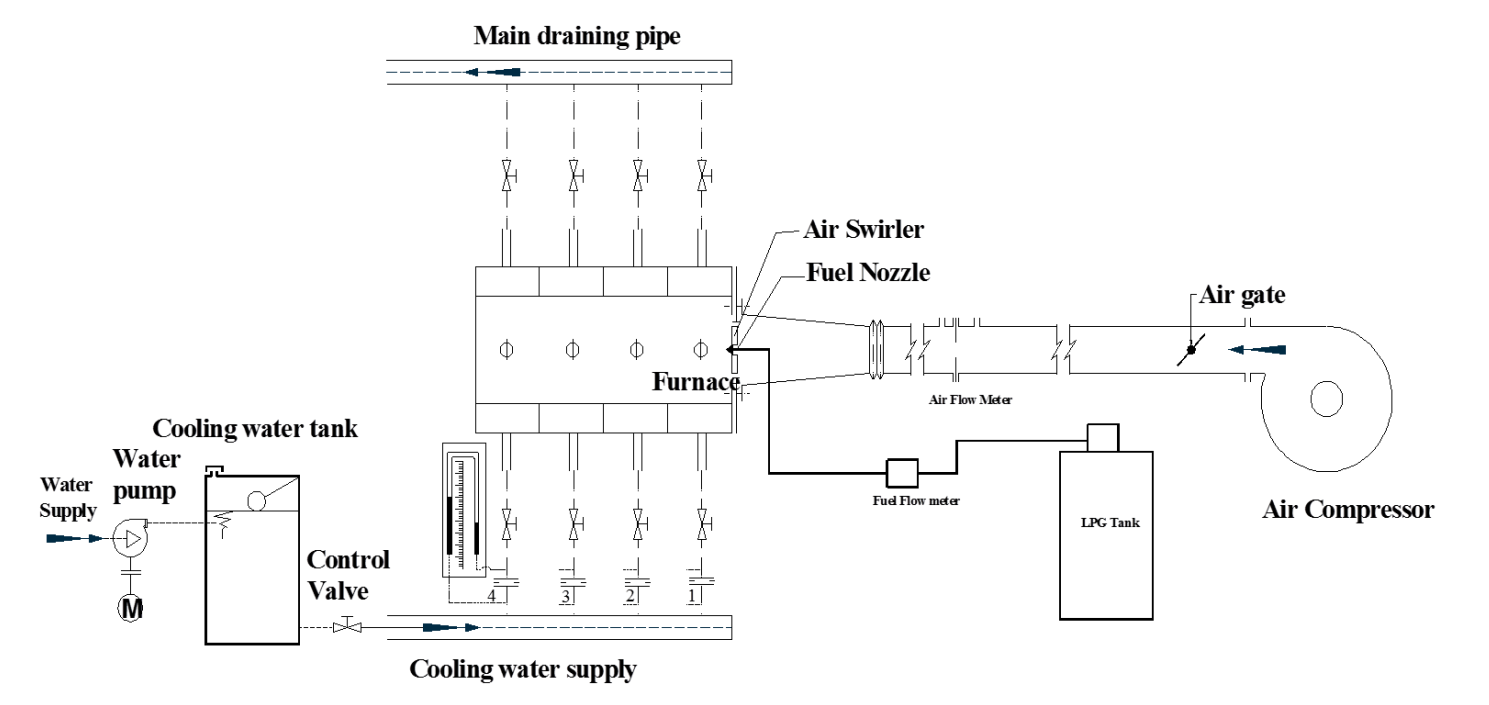


Fig. 1: Test Rig Schematic Diagram

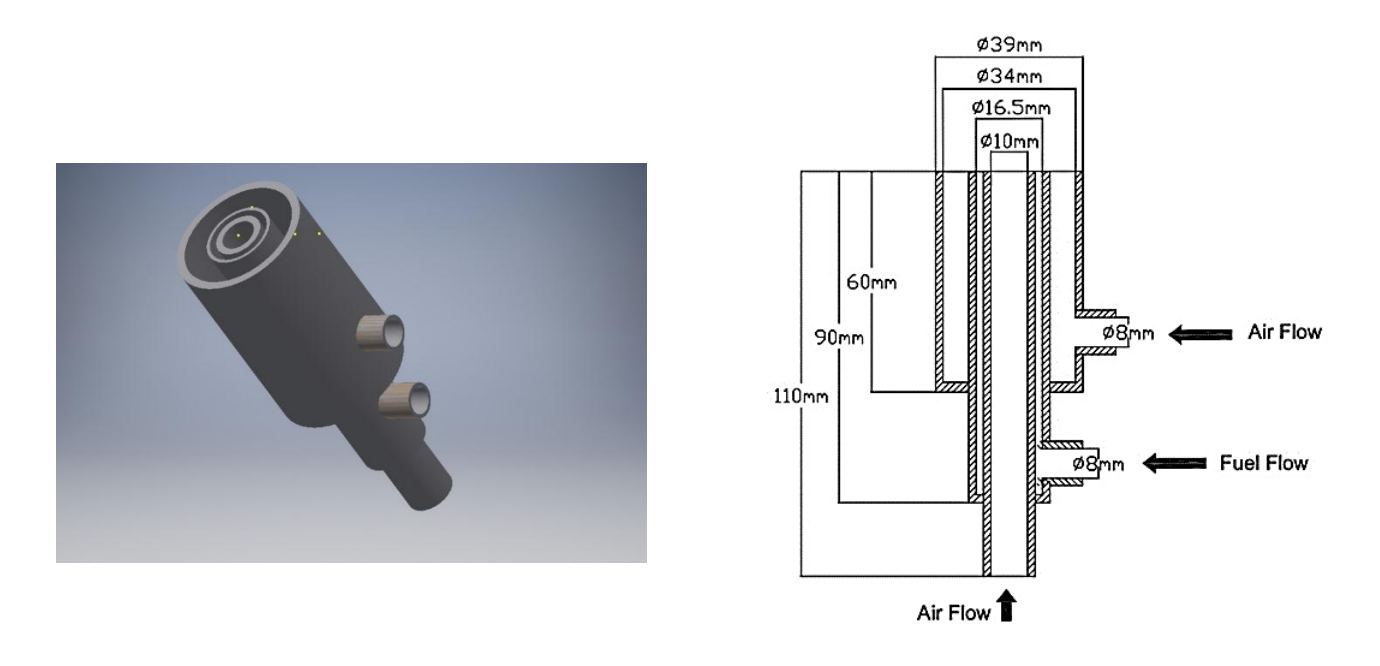


Fig. 2: Concentric inverse and normal diffusion flames (CINDF) burner

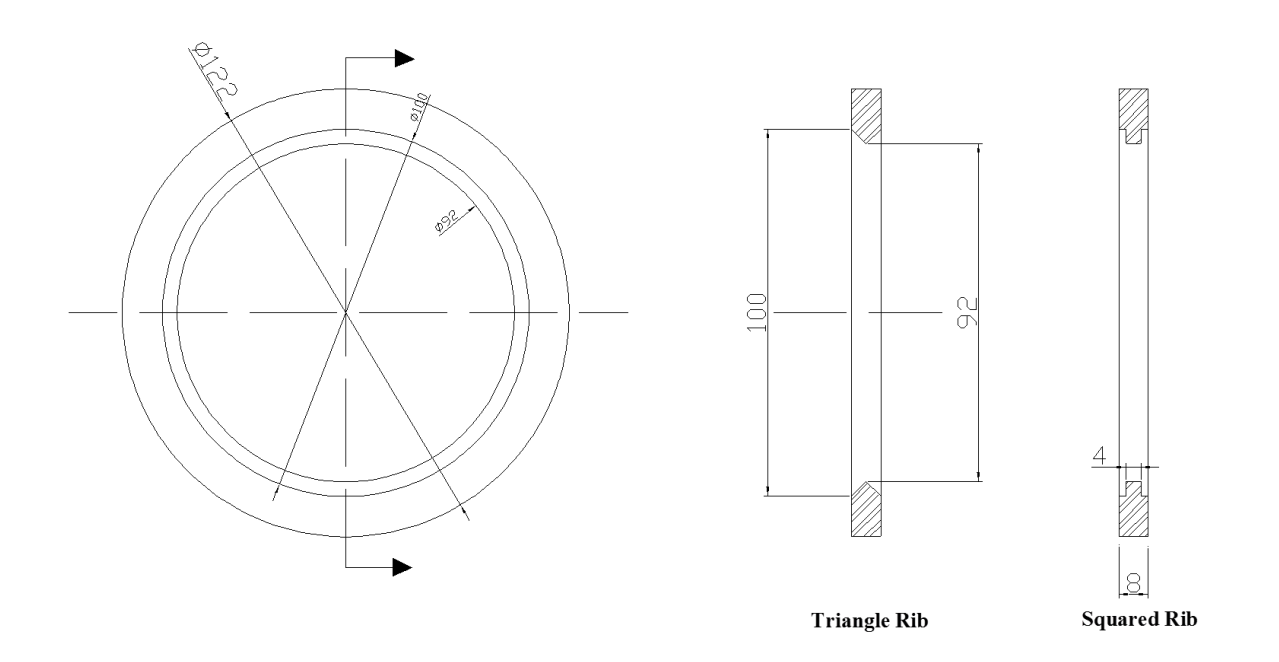


Fig. 3: Triangle and Squared Rib Geometry

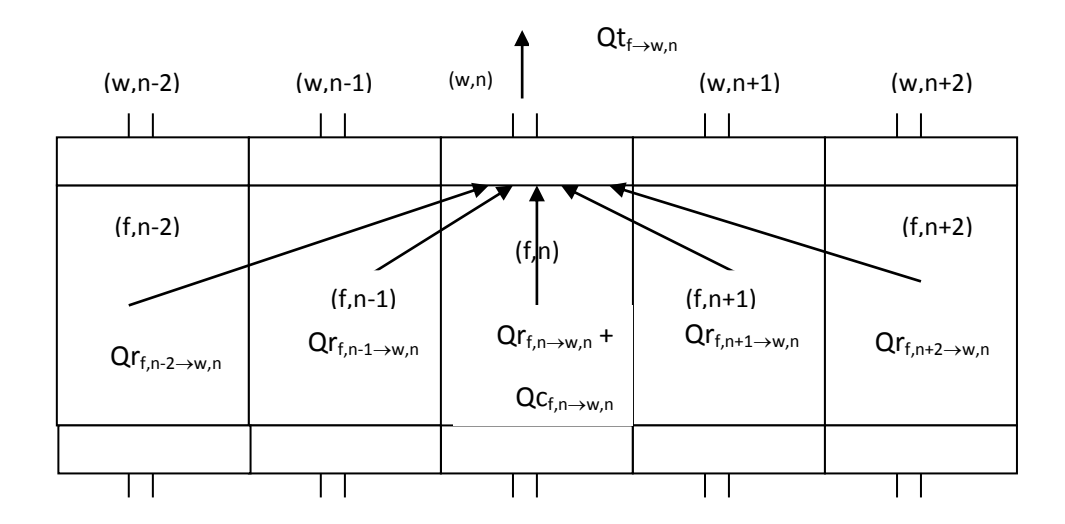


Fig. 4: Schematic Diagram Showing the Heat Transfer to the Furnace Wall Segment (w,n)

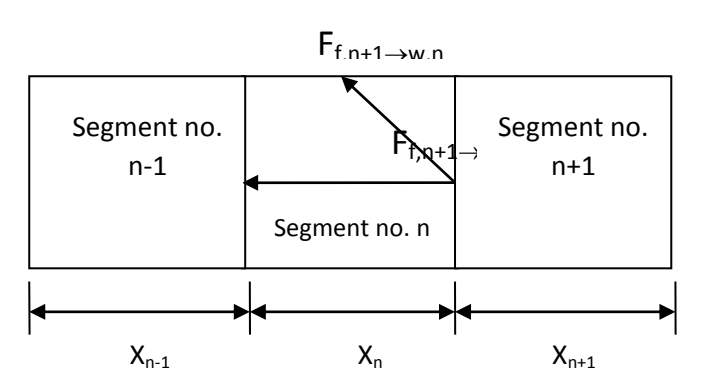


Fig. 5: Schematic Diagram for the view factor

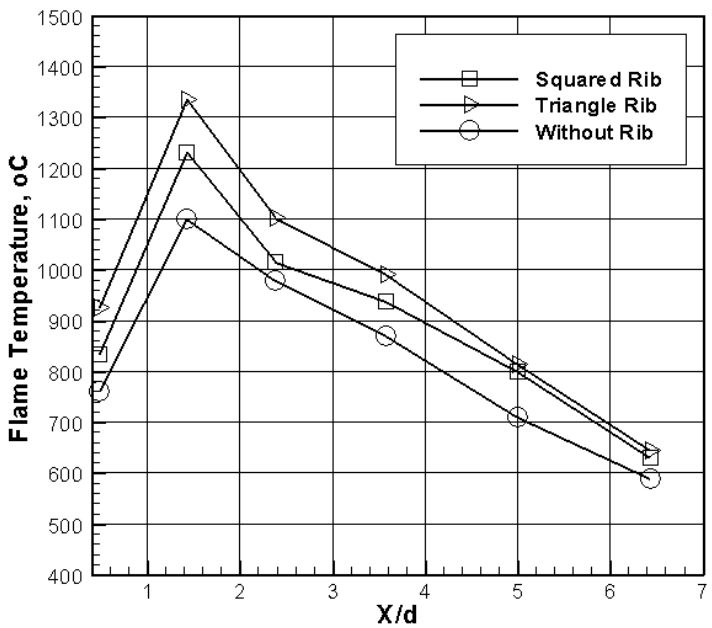


Fig. 6: Variation of the flame temperature along the furnace for premixed flame burner

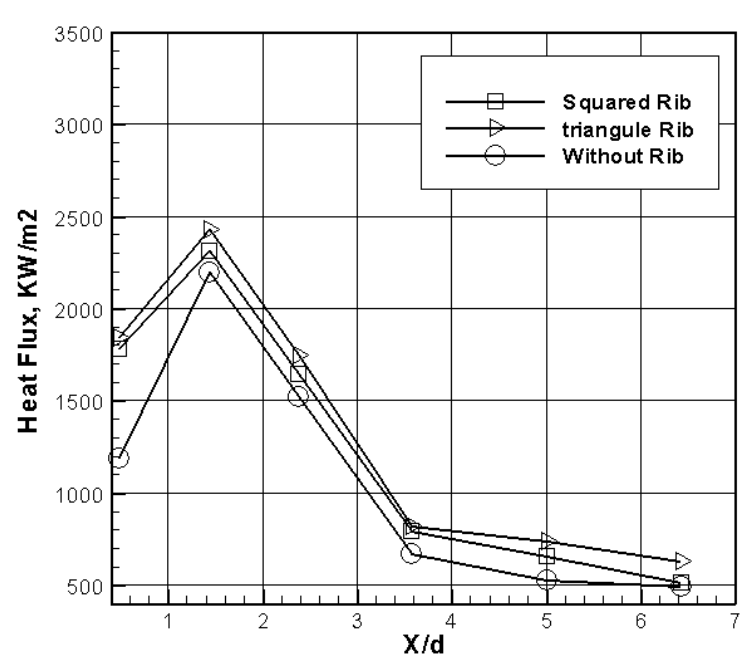


Fig. 7: Variation of the heat flux along the furnace for premixed flame burner

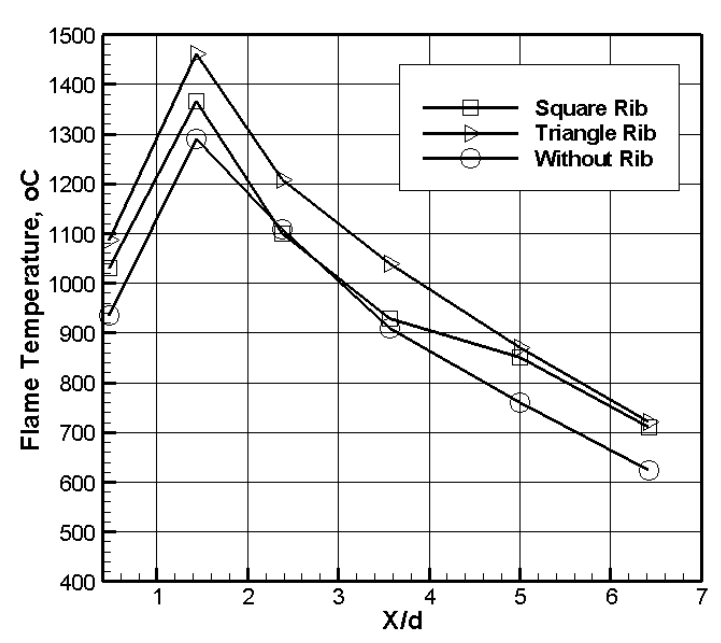


Fig. 8: Variation of the flame temperature along the furnace for CINDF flame burner

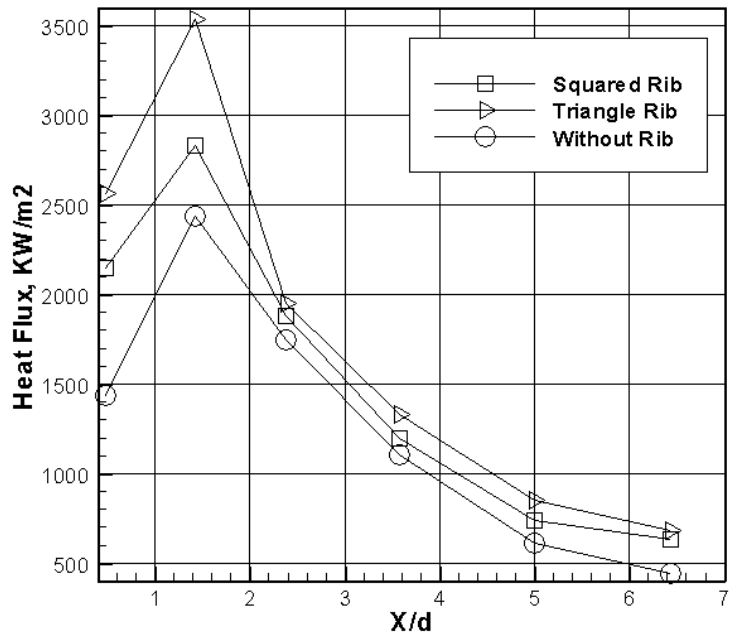


Fig. 9: Variation of the heat flux along the furnace for CINDF flame burner

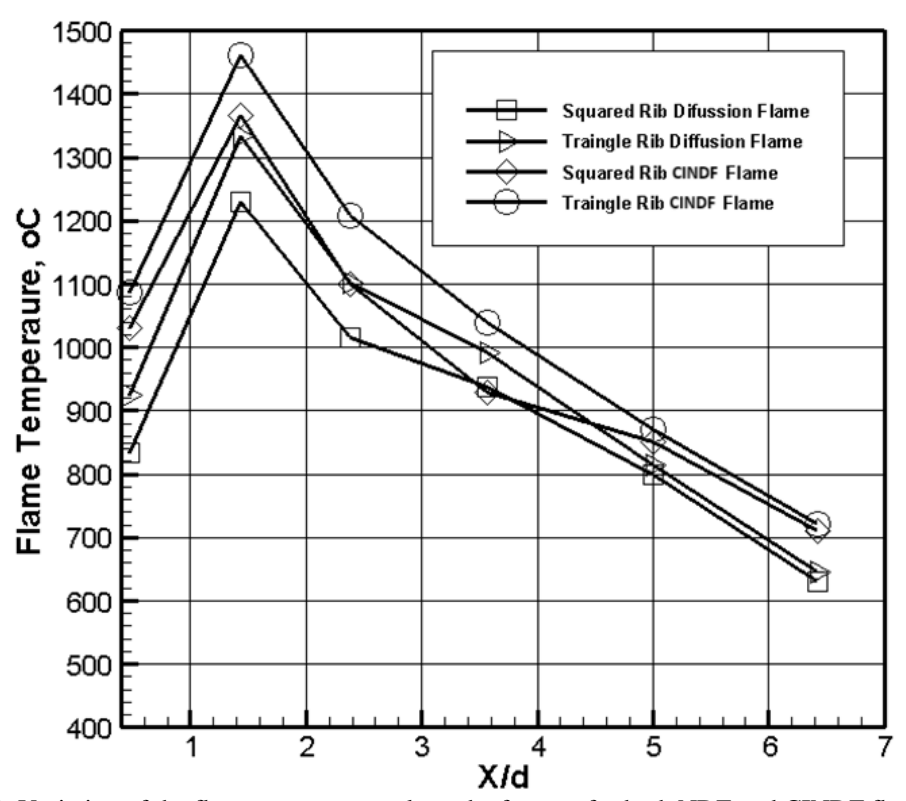


Fig. 10: Variation of the flame temperature along the furnace for both NDF and CINDF flame burner

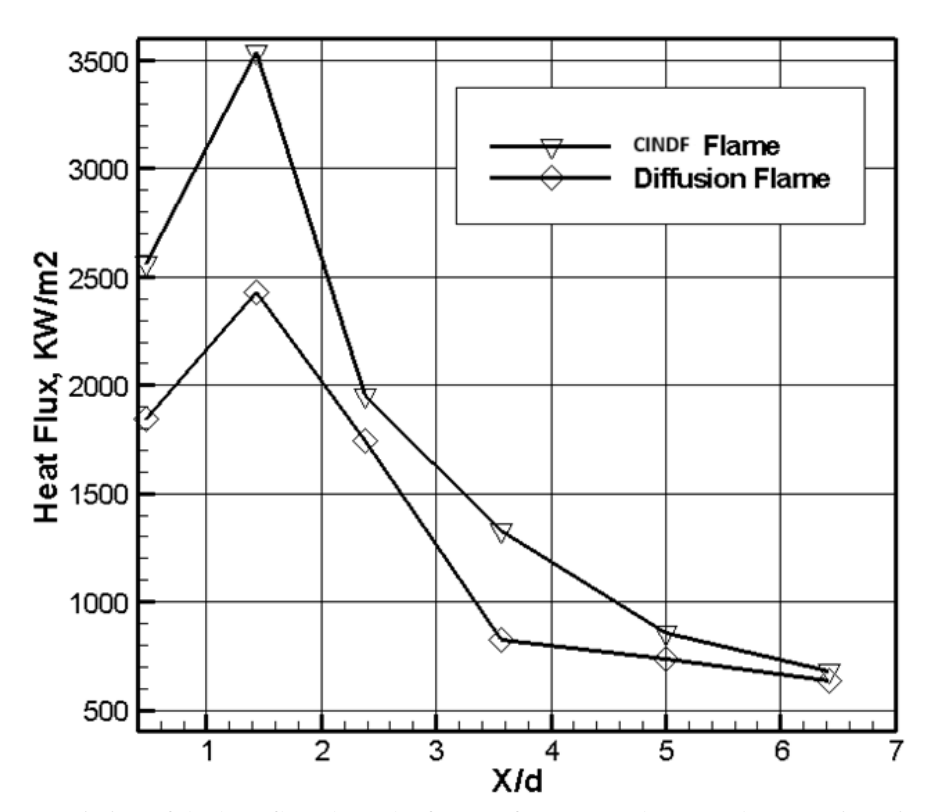


Fig. 11: Variation of the heat flux along the furnace for NDF and CINDF burner using triangle rib

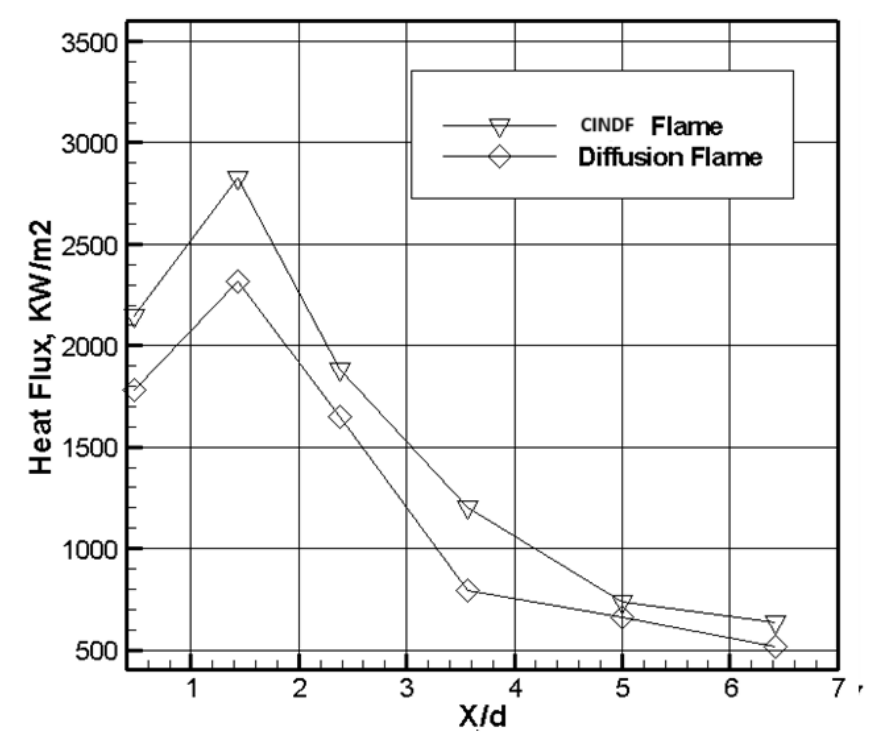


Fig. 12: Variation of the heat flux along the furnace for CINDF and NDF burner using square rib

Comparison between the effect of inserting squared and triangle rib CO emissions

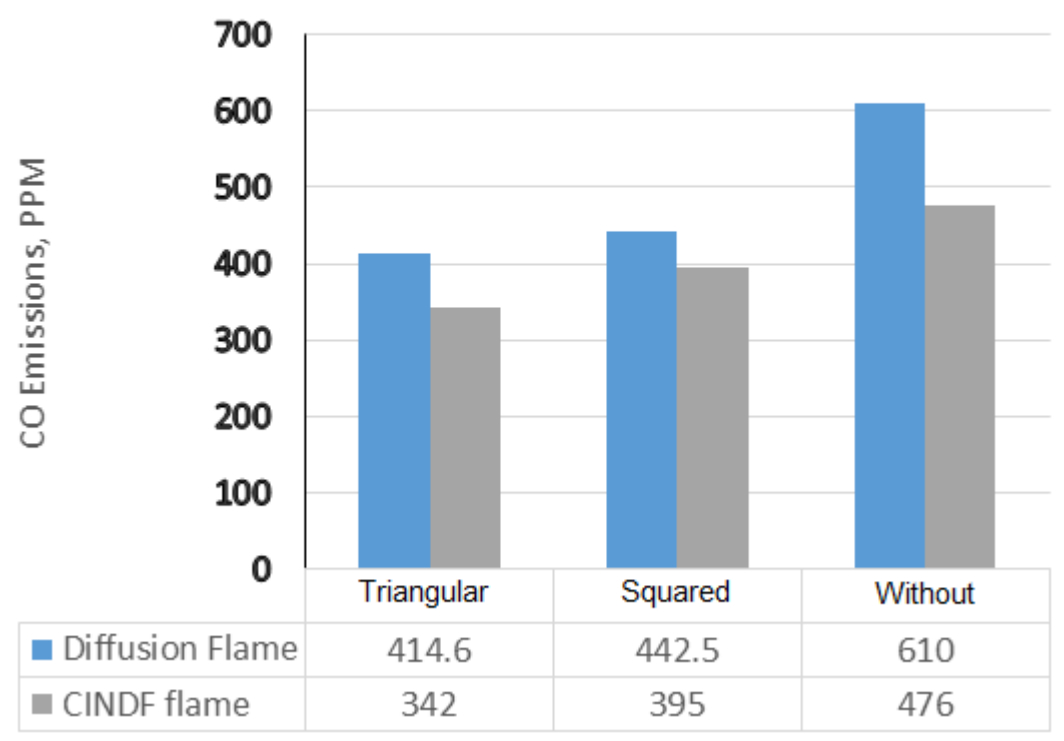


Fig. 13: Comparison between the effect of inserting squared and triangular rib CO emissions

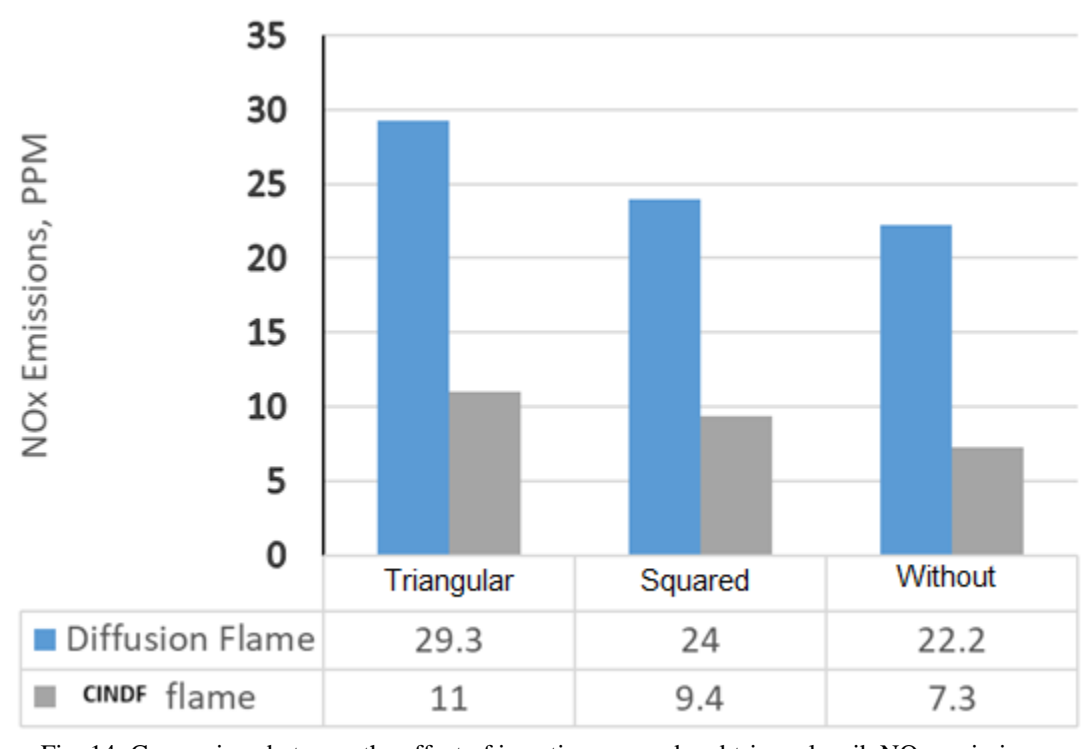


Fig. 14: Comparison between the effect of inserting squared and triangular rib NOx emissions

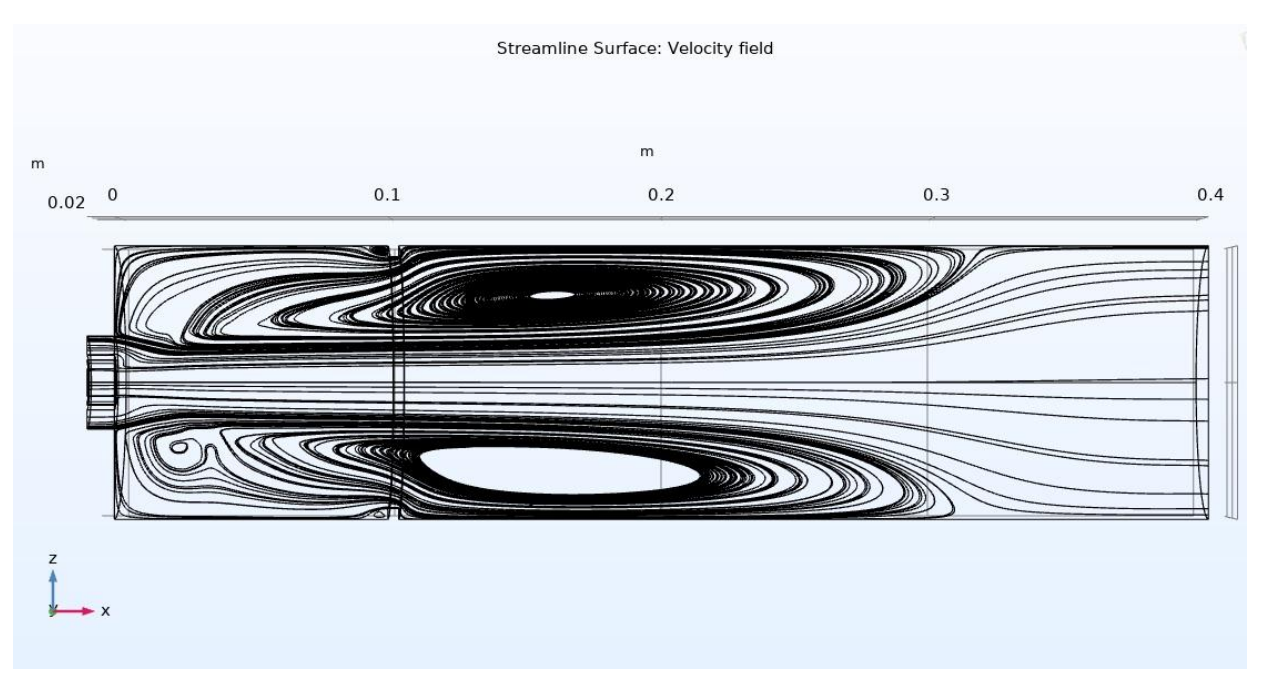


Fig. 15: Variation of velocity field in case of using annular ribs

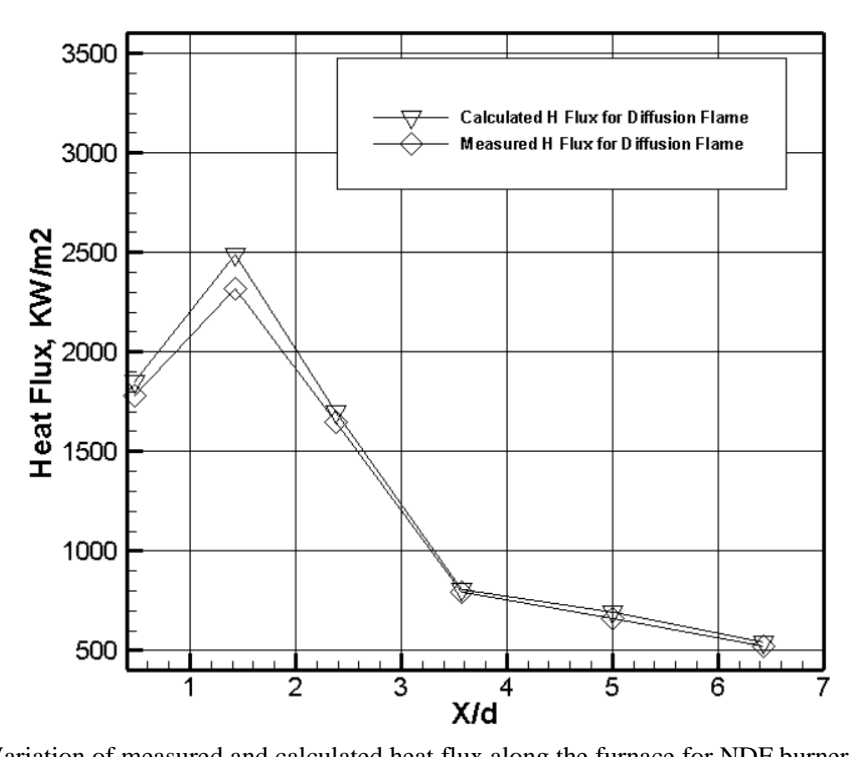


Fig. 16: Variation of measured and calculated heat flux along the furnace for NDF burner without rib

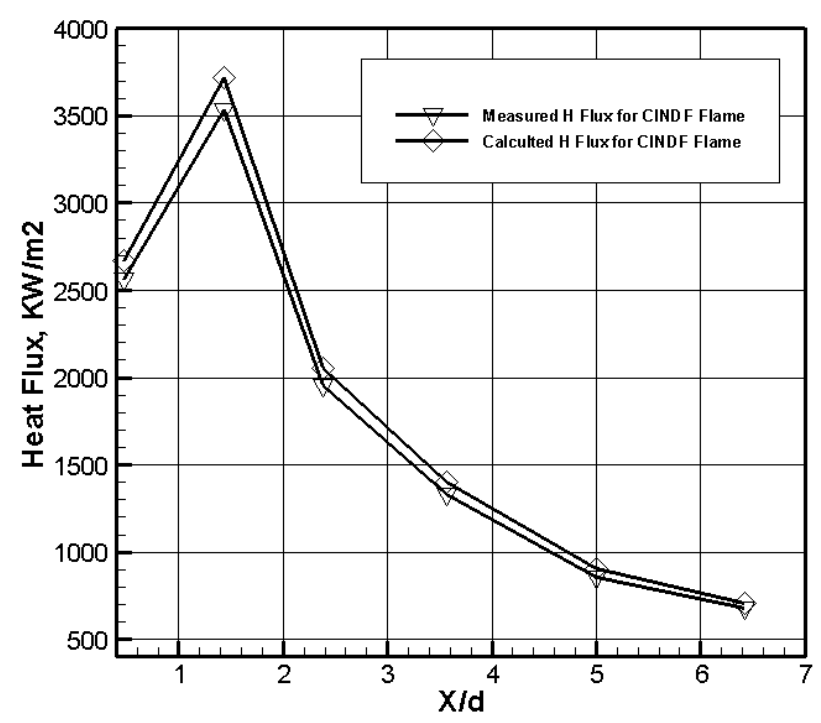


Fig. 17: Variation of the measured and calculated heat flux along the furnace for CINDF burner without rib

NOMENCLATURES

F

 A_f : The furnace inner cross sectional ares.

A_w : The furnace inner wall surface area, m².
C : The water specific heat, 4.18 kJ/kg °C.
D : The furnace internal diameter, m .

The view factor between the flame and

wall segment, dimensionless.

 h_c : The convective heat transfer coefficient, $W/(m^2\,^{\circ}C)$.

X/D : Dimensionless furnace length, dimensionless.

X : Furnace axial distance, m.

m°_w : Cooling water mass flow rate, kg/s.

 $Qt_{f\rightarrow w.n}$: tal rate of heat absorbed by the wall segment number (n), kW.

 $Qr_{f,n\to w,n}$: The rate of heat transfer from the flame segment number (n) to the wall

segment number (n) by radiation, kW.

 $Qc_{f,n\to w,n} \hspace{1cm}$: The rate of heat transfer from the flame segment number (n) to the wall

segment number (n) by convection, kW.

 $Qr_{fn+1\to w,n}$: The rate of radiative heat transfer from the flame segment number (n+1)

to the wall segment number (n), kW.

 $Qr_{f,n+2 \to w,n}$: The rate of radiative heat transfer from the flame segment number (n+2)

to the wall segment number (n), kW.

 $Qr_{f,n-1 o w,n}$: The rate of radiative heat transfer from the flame segment number (n-1) to

the wall segment number (n), kW.

 $Qr_{f,n\text{-}2\to w,n}$: The rate of radiative heat transfer from the flame segment

mber (n-2) to the wall segment number (n), kW.

 q_n : The heat flux for wall number n, kW/m^2 .

 $\begin{array}{lll} T_f & : & Flame \ temperature, \ K. \\ T_w & : & Wall \ temperature, \ K. \end{array}$

 $\begin{array}{lll} \epsilon_{w.n} & : & Wall \ emissivity \ at \ segment \ n. \\ \epsilon_{f,n} & : & Flame \ emissivity \ at \ segment \ n. \end{array}$

φ : Equivalence ratio, dimensionless which is the ratio between the

stoichiometric air to fuel ratio to the actual air to fuel ratio.

REFRENCES

- [1] Al-Shamani A. N., Sopian K, M., H. A. and SohifMat, 2015, Enhancement heat transfer characteristics in the channel with trapezoidal rib—groove using Nano fluids, Case Studies in Thermal Engineering, Vol. 5, p. 48-58.
- [2] Amr A. A., Ali E., Mahmoud K., Hany E. A. E. S., 2017, The Effect of Varying Location and the Shape of the Annular Ribs on the Combustion Characteristics and Heat Transfer for Premixed Flame, International Journal of Innovative Research in Science, Engineering and Technology, Vol. 6, Issue 6.
- [3] Anand M. S. and Gouldin F. C., 1985, Combustion Efficiency of a Premixed Continuous Flow Combustor, Journal of Engineering for Gas Turbine and Power, Vol. 107.
- [4] Artur B., Wojciech N., 2015, Heat transfer behavior inside a furnace chamber of large-scale supercritical CFB reactor, International Journal of Heat and Mass Transfer, Vol. 87, p. 464-480
- [5] Bodade, Pradip R., 2013, A study on the heat transfer enhancement for air flow through a duct with various ribs inserts, International Journal of Latest Trends in Engineering and Technology, Vol. 2 Issue 4.
- [6] Boonloi A., Jedsadaratanachai W., 2022, Numerical predictions of flow topology and heat transfer in a square duct with staggered V-ribs, International Communications in Heat and Mass Transfer, Vol. 139, 106483
- [7] Bradly D. and Matthews K. J., 1968, Measurement of high gas temperature with fine wire thermocouples, Journal of Mechanical Engineering Science, Vol. 10, p. 299-305.
- [8] Caliskan S., Baskaya S., 2012, Velocity field and turbulence effects on heat transfer characteristics from surfaces with Vshaped ribs, Int. J. Heat Mass Transfer, Vol. 55, p. 6260–6277.
- [9] Caliskan, 2013, Flow and heat transfer characteristics of transverse perforated ribs under impingement jets, International Journal of Heat and Mass Transfer, Vol. 66, p. 244-260
- [10] D'Anna A., 2009, Combustion-formed nanoparticles, Proceedings of the Combustion Institute Vol. 32, p. 593–613.
- [11] El-Mahallawy F. M., 2002, Fundamentals and Technology of Combustion, El Sevier Science Ltd., First Edition.
- [12] Ernest O. D., 1983, Measurement Systems Application and Design, McGraw- Hill International Book Company, Third Edition,
- [13] Hassanin S. H., 2001, Augmentation of Emission Characteristics of Liquid Fuel Flames, Ph.D Thesis, Faculty of Engineering, Ain Shams University, Cairo, Egypt,

- [14] Hisham E., Xiaobing Z., Mohammed N. G. and Mozdalifah A., 2022, Heat transfer enhancement of hydrogen rocket engine chamber wall by using V-shape rib, International Journal of Hydrogen Energy, Vol. 47, Issue 16, p. 9775-9790
- [15] Holman J. P., 1981, Heat Transfer, McGraw-Hill International Book Company, Fifth Edition.
- [16] Hottel H. C., Sarofim A. F., 1967, Radiative Transfer, Mc Graw-Hill Book Company, New York.
- [17] Kamal M. M. 2013, A comparative study of the port geometrical effects on sharp corners' jet triple flames, Experimental Thermal and Fluid Science, Vol. 51, p. 149-163
- [18] Kamali, Binesh, 2008, The importance of rib shape effects on the local heat transfer and flow friction characteristics of square ducts with ribbed internal surfaces, International Communications in Heat and Mass Transfer, Vol. 35, Issue 8, p. 1032-1040.
- [19] Kline S. J., McClintock F. A, 1953, Describing uncertainties in single sample experiments, Mech Eng; 75:3–8.
- [20] Kotb A., Kamal M. M., Baghdady A., Hany S., 2022, Case study for swirling flow and porous media on triple coaxial ports inverse diffusion flame" Alexandria Engineering Journal, Vol. 61, Issue 3, p. 2294-2306
- [21] Phillips H., 1965, Flame in a buoyant methane layer, Symposium (International) on Combustion, Vol. 10, Issue 1, p. 1277-1283.
- [22] Siliang N., Dan Z., Yancheng Y., Yue H., Bin W., and Yunpeng S., 2021, NOx emission and energy conversion efficiency studies on ammonia-powered micro-combustor with ring-shaped ribs in fuel-rich combustion, Journal of Cleaner Production, Vol. 320, 128901
- [23] Suze L. K., 2007, Thermal and Emission characteristics of an inverse diffusion flame with Circumferentially arranged fuel ports, Ph.D thesis, The Hong Kong Polytechnic University.
- [24] Vander W. R. L, Jensen K. A. and Choi M. Y., 1997, Simultaneous laser-induced emission of soot and polycyclic aromatic hydrocarbons within a gas-jet diffusion flame, Combustion and Flame Vol. 109, p. 399–414.
- [25] Xiao Z., Joseph D. C., and Elaine S. O., 2022, Triple flames in swirling flows, Combustion and Flame, Vol. 245, 112364
- [26] Ahmed Ibrahim Khalil, Mahmoud K., Hany E. A. E. S., 2017, Enhancement of combustion characteristics and heat transfer by using annular ribs for the triple flame, International Journal of Innovative Research in Science, Engineering and Technology, Vol. 6, Issue 6.